

See discussions, stats, and author profiles for this publication at: <https://www.researchgate.net/publication/215631509>

Heat Capacity of Silk Fibroin Based on the Vibrational Motion of Poly(amino acid)s in the Presence and Absence of Water

ARTICLE *in* MACROMOLECULES · JULY 2008

Impact Factor: 5.8 · DOI: 10.1021/ma8003357

CITATIONS

24

READS

101

3 AUTHORS:



M. Pyda

University of Tennessee

111 PUBLICATIONS 1,849 CITATIONS

SEE PROFILE



Xiao Hu

Rowan University

79 PUBLICATIONS 2,879 CITATIONS

SEE PROFILE



Peggy Cebe

Tufts University

248 PUBLICATIONS 4,671 CITATIONS

SEE PROFILE

Heat Capacity of Silk Fibroin Based on the Vibrational Motion of Poly(amino acid)s in the Presence and Absence of Water

M. Pyda,^{*,†,‡,§} Xiao Hu,[§] and Peggy Cebe^{*,§}

Department of Chemistry, The University of Technology, Rzeszow, 35959 Rzeszow, Poland;
ATHAS-MP, 1608 Bexhill Dr., Knoxville, Tennessee 37922; and Department of Physics and Astronomy,
Tufts University, STC-208, 4 Colby Street, Medford, Massachusetts 02155

Received February 14, 2008; Revised Manuscript Received May 9, 2008

ABSTRACT: The heat capacities in the solid state, below the glass transition, of *Bombyx mori* silk fibroin with and without water have been determined based on the contribution of vibrational motions of the components: poly(amino acid)s and water. These vibrational heat capacities were constructed using the Advanced Thermal Analysis System (ATHAS) Data Bank. The heat capacities, C_p , of dry silk and silk–water were linked to their vibrational spectra based on the group and skeletal vibration contributions. For dry silk, the experimental and calculated C_p agree to better than $\pm 3\%$ between 200 and 435 K. The heat capacity of the solid silk–water system, below the glass transition, was estimated from a sum of linear combinations of the molar fractions of the vibrational heat capacities of dry silk and glassy water. The approach presented allows one to predict the low-temperature vibrational heat capacity for dry silk and for the silk–water system down to 0 K and, together with an extension to higher temperatures, above the glass transition. This can be used as a reference baseline for quantitative thermal analysis of this biomaterial.

I. Introduction

Proteins, whether specially synthesized or found in nature, are generally large and complex macromolecules with molecular weights ranging from 10^3 Da (e.g., insulin) to 10^6 Da (e.g., titin). The effect of temperature on protein molecules is an important topic in the study of protein function. By simply adjusting the temperature, the protein structure can be dramatically changed, affecting their final biofunctions. However, for researchers studying complicated proteins, separate thermal studies based on each individual protein structure will be time-consuming. This problem led us to think about whether there is a practical way to use the thermal properties of the basic amino acids to predict the thermal properties of the large complicated proteins, which idea has been similarly developed in the study of DNA molecules. This process will launch our thermal analysis study of protein structure and function, taking it from a simple repeated experimental level to a theoretical model level, which can be extremely useful for the design of new, as yet unknown, protein structures.

Predicting the physical properties of protein macromolecules is an important challenge for protein scientists. Fortunately, the amino acid constituents of the proteins are few in number, and for many physical properties a simple additivity rule may be employed to predict the behavior of the macromolecule. The bulk property, P , of the large macromolecule can be written by using a linear combination of small constituent properties, p , as $P = \sum_i N_i p_i$, where N_i is the number of units (here, amino acid residues) characterized by property p_i . In this work, we investigate the additivity rule for the vibrational heat capacity of a large biomacromolecule, specifically silk fibroin, in the presence and absence of water by direct calculation and then compare these computations to experimentally measured heat capacity data.

Bombyx mori silk fibroin is used here as an exemplar of the class of fibrous proteins, of interest in the investigation of

biological systems.^{1–5} The silkworm's natural silk fiber has been extensively studied as an interior structural protein with water and with water removal processes for many biomaterials applications.^{6–10} Silkworm-domestic *B. mori* silk fibroin analyzed for protein composition and the complete sequence of amino acids has been reported by Kaplan and co-workers.^{1,2} Detailed contents of mol % of amino acid compositions are presented in Table 1. Studies show two primary regions of the protein: the fibroin heavy chain (around 391.6 kDa) and light chain (around 27.7 kDa) components.¹¹

A fuller understanding of biomacromolecules such as *Bombyx mori* silk fibroin requires knowledge of their structure and energetics. The structure of silk fibroin has been reported relatively thoroughly as silk I, II, and III.^{13,14} Silk I is the water-soluble structure existing before the spinning process. Silk II is the insoluble extended β -sheet conformation crystal formed after spinning of silk fibers from the spinneret of the silkworm. The transition from silk I to silk II occurs during the spinning of the silk fiber.

The energetics of silk fibroin can be determined by thermal analysis. Many reports of measurements of thermal properties of silk are available in the literature,^{15–19} but little quantitative information and quantitative interpretation of the existing data on the microscopic level is currently available. However, pioneering work in the quantitative thermal analysis of the pure biomaterial and partially hydrated silk has been initiated by Cebe and co-workers.^{20–25} In order to fully understand the formation of silk fibroin and for the evaluation of the thermodynamic processes, a proper link had to be established between the macroscopic properties and the microscopic structure and behavior. For example, the apparent heat capacity of silk fibroin with water has a complicated temperature dependence that is difficult to interpret without considering the molecular motions of poly(amino acid)s and water.^{20,21,25}

The interaction between silk and water molecules on a microscopic level can be investigated by proton NMR²⁶ and FTIR^{20,25} intensity measurements. On a macroscopic scale, differential scanning calorimetry (DSC), temperature-modulated DSC (TMDSC), and adiabatic calorimetry are widely used for characterization of the thermal properties such as heat capacity

* Corresponding authors. E-mail: mpyda@utk.edu; peggy.cebe@tufts.edu.

† The University of Technology.

‡ ATHAS-MP.

§ Tufts University.

and phase transitions over a whole range of temperatures.^{27–31} Traditionally, the low-temperature heat capacity of biomacromolecules and macromolecules are measured by adiabatic calorimetry to establish a baseline vibrational heat capacity to be used for quantitative thermal analysis. However, the quest for more rapid, economical ways to perform this vibrational heat capacity baseline has directed interest to alternative approaches. This is the case not only for silk but also for future work with other pertinent biomacromolecules such as collagen, which enjoys much attention.^{32,33} The methods presented here are based on the vibrational heat capacities for the individual amino acids, which we took from the ATHAS Data Bank.³⁴ This has proved to be a useful approach to quickly and quantitatively examine the thermal properties of many biomacromolecules.

In the present paper, we report on calculations that enable us to interpret the experimental data of the heat capacity of dry silk fibroin and the partially hydrated silk–water system in terms of the vibrational motions of silk and water. The heat capacity from low temperatures to the glass transition region of dry silk and silk–water were linked to the vibrational spectra of the poly(amino acid)s and glassy water as found in the ATHAS Data Bank.³⁴ The total vibration heat capacity of silk was calculated as a sum of a linear combination of the vibration heat capacity of the individual poly(amino acid) residues collected in database.³⁴ Furthermore, this total vibrational heat capacity of silk and the silk–water system has been extended to high temperatures and serves as the baseline for quantitative thermal analysis within the transition regions.

Calculation of the Heat Capacity for the Solid State of Dry Silk and Water. Determination of heat capacity in the solid state of silk and silk–water system from 0 K to the glass transition region ($T_g = 178$ °C for dry silk fibroin^{35,36}) is based on the common acceptable assumption that contributions to the heat capacity come only from vibrational motions of silk and water. First, the total solid vibrational heat capacity of dry silk, C_p^{silk} , is constructed as a sum of products of the vibrational heat capacity of the individual poly(amino acid) residues, $C_p(i)$, and the total number of each kind found in the complete sequence of amino acids in the silk fibroin macromolecule. This can be written as

$$C_p^{\text{silk}} = N_{\text{Gly}}C_p(\text{Gly}) + N_{\text{Ala}}C_p(\text{Ala}) + \cdots + N_{\text{Met}}C_p(\text{Met}) \\ = \sum_i N_i C_p(i) \quad (1)$$

where N_i is total number of each type of amino acid as found in ref 11 and also can be calculated from

$$N_i = X_i \frac{M_w(\text{silk})}{M_w(i)} \quad (2)$$

where X_i represents the molar fraction of each type of amino acid which contributes to *Bombyx mori* silk fibroin, $M_w(\text{silk})$ is the total molecular weight mass of silk, and $M_w(i)$ is the molecular weight mass of each kind of amino acid, $i = \text{Gly, Ala, Ser, } \dots, \text{Met}$, according to the notation in Table 1. Note that $M_w(i)$ is the molecular weight mass of the repeating unit of poly(amino acid)s rather than of the amino acid's small molecule. For example, the molecular weight mass of the repeating unit of Alanine (Ala) is 71.08 g/mol (see Table 1). Heat capacity, $C_p(i)$, is the vibrational heat capacity of the repeating unit of the i th kind of poly(amino acid) in the solid state which is collected, and available, in the ATHAS Data Bank for biomaterials.³⁴ The numbers, N_i , and compositions of the amino acids in silk fibroin were obtained from the Swiss-Prot protein sequence database¹¹ and from ref 2 and also are presented in Table 1.

The computation of the vibrational heat capacity of each poly(amino acid) and water is based on the advanced method used for synthetic polymers from the well-established ATHAS scheme.^{34,37} Briefly, a general scheme of this computation is presented below. The vibrational spectra of the solid state of each kind of poly(amino acid), consisting of $3N$ vibrators, with N describing the total numbers of atoms in the repeating unit of the poly(amino acid), can be separated into group and skeletal vibrations ($3N = N_{\text{gr}} + N_{\text{sk}}$). The numbers and types of group vibrations (N_{gr}) are derived from the chemical structure of the sample as a series of single frequencies and box frequencies over narrow frequency ranges. These frequencies can be evaluated from normal-mode calculations on repeating units of the poly(amino acid)s based on a fit to experimental infrared and Raman frequencies or from suitable low molar mass analogues. All approximate group vibrational frequencies of the poly(amino acid)s that are relevant to silk have been collected from the ATHAS Data Bank and from the literature.^{34,37–39}

The skeletal vibrations (N_{sk}) are not represented very well by normal-mode calculations but can be approximated by Debye's approach.⁴¹ For small molecules in the solid state these vibrations are well described by a three-dimensional Debye approach.⁴¹ On the other hand, for linear polymeric materials the experimental low-temperature heat capacities are approximated by linear combinations of one-, two-, and three-dimensional Debye functions using the general Tarasov equation.^{37,40,42} In order to obtain this Debye-like contribution, which we will henceforth call the skeletal vibrational heat capacity, first, the experimental heat capacities at constant pressure

Table 1. Amino Acids Comprising *Bombyx mori* Silk Fibroin and Their Parameters¹²

amino acid	M_w molar mass [g/mol]	no. of heavy chain amino acids	no. of light chain amino acids	N_i total no. of amino acids	mol % in silk ^a
glycine (Gly)	57.05	2415	22	2437	42.9
alanine (Ala)	71.08	1593	37	1630	30.0
serine (Ser)	87.08	635	25	660	12.2
tyrosine	163.18	277	11	288	4.8
aspartic acid/asparagine	137.07	25	17	42	1.9
arginine	192.65	14	10	24	0.5
histidine	137.15	5	5	10	0.5
glutamic acid/glutamine	167.125	30	5	35	1.4
lysine	163.63	12	5	17	0.4
valine	99.14	97	19	116	2.5
leucine	113.17	7	20	27	0.6
isoleucine	113.17	13	21	33	0.6
phenylalanine	147.18	29	8	37	0.7
proline	114.02	14	9	23	0.5
threonine	101.11	47	8	55	0.9
methionine (Meth)	131.20	4	2	6	0.1

^a Reference 2.

$C_p(\text{exp})$, should be converted into heat capacities at constant volume, $C_V(\text{exp})$, using the standard thermodynamic relationship^{28,37}

$$C_p = C_V + TV \frac{\alpha^2}{\beta} \quad (3)$$

where T is temperature, V is volume, and α and β are the coefficients of thermal expansion and compressibility, respectively. They should be considered as functions of temperature. In case α and β are not available, the heat capacity can be estimated using the Nernst–Lindemann approximation:^{28,37}

$$C_p - C_V = 3RA_0 \frac{C_p^2}{C_V} \frac{T}{T_m} \quad (4)$$

where R is the universal gas constant, A_0 equals 3.9×10^{-3} (mol K/kJ), and T_m is the equilibrium melting temperature. For sufficiently low temperatures, the experimental heat capacity, C_V , contains only vibrational contributions and can be separated into the heat capacities coming from group, $C_V(\text{group})$, and skeletal, $C_V(\text{skeletal})$, vibrations:

$$C_V = C_V(\text{group}) + C_V(\text{skeletal}) \quad (5)$$

The heat capacity from the group vibrations, $C_V(\text{group})$, of the poly(amino acid)s was estimated by the sum of the heat capacity from a series of single and box frequencies and is written as

$$C_V(\text{group}) = C_V(\text{Einstein}) + C_V(\text{box}) \quad (6)$$

To evaluate the heat capacity from group vibrations, we evaluate each term on the right-hand side, using eqs 7 and 8. The heat capacity from single frequencies arising from normal modes (Einstein modes) is given by a sum of the Einstein function:

$$C_V(\text{Einstein})/NR = \sum_i E(\Theta_{Ei}/T) = \sum_i \frac{(\Theta_{Ei}/T)^2 \exp(\Theta_{Ei}/T)}{[\exp(\Theta_{Ei}/T) - 1]^2} \quad (7)$$

where the summation takes place on the individual modes, $\Theta_{Ei} = h\nu_i/k$ is the Einstein frequency in kelvin, and h and k are the Planck and Boltzmann constants, respectively. The heat capacity of a box distribution, $C_V(\text{box})$, is given by a boxlike spectrum and each box is represented by a sum of one-dimensional Debye functions, \mathbf{D}_1 , for the sets of vibrations within the frequency interval from Θ_L to Θ_U :^{28,37,42}

$$C_V(\text{box})/NR = B(\Theta_U/T, \Theta_L/T) = \frac{\Theta_U}{\Theta_U - \Theta_L} [\mathbf{D}_1(\Theta_U/T) - (\Theta_L/\Theta_U) \mathbf{D}_1(\Theta_L/T)] \quad (8)$$

where $\Theta_L = h\nu_L/k$ is the lower frequency and $\Theta_U = h\nu_U/k$ is the upper frequency, in kelvin, in the boxlike spectrum.

$C_V(\text{skeletal})$ from eq 5 is calculated by subtracting $C_V(\text{group})$ from C_V . Then $C_V(\text{skeletal})$ is fitted to the general Tarasov function \mathbf{T} :^{28,37,42}

$$\begin{aligned} C_V(\text{skeletal})/N_{\text{sk}}R &= \mathbf{T}(\Theta_1/T, \Theta_2/T, \Theta_3/T) \\ &= \mathbf{D}_1(\Theta_1/T) - (\Theta_2/\Theta_1) [\mathbf{D}_1(\Theta_2/T) - \mathbf{D}_2(\Theta_2/T)] - \\ &\quad (\Theta_3^2/\Theta_1\Theta_2) [\mathbf{D}_2(\Theta_3/T) - \mathbf{D}_3(\Theta_3/T)] \end{aligned} \quad (9)$$

The three characteristic Debye temperatures Θ_1 , Θ_2 , and Θ_3 for each poly(amino acid) of silk fibroin that represent the maximum frequencies of the corresponding distribution of the density of states are obtained from the best fit of experimental data to eq 9. In eq 9 the theta-temperatures are such that $\Theta = h\nu/k$ with the Debye frequencies expressed in kelvin. The functions \mathbf{D}_1 , \mathbf{D}_2 , and \mathbf{D}_3 are the one-, two-, and three-

dimensional Debye functions, respectively,^{28,40,41} and represent heat capacity in the form

$$C_V/NR = D_i(\Theta_i/T) = i(T/\Theta_i)^i \int_0^{\Theta_i/T} \frac{(\Theta/T)^{i+1} \exp(\Theta/T)}{[\exp(\Theta/T) - 1]^2} d(\Theta/T) \quad (10)$$

where i is equal to 1, 2, or 3. In eq 10, N denotes the number of the vibrational modes for a given Debye frequency distribution. Figure 1a shows a scheme of the distribution of the density of states for Debye frequencies of the skeletal modes. The temperature Θ_3 describes skeletal contributions with a quadratic frequency distribution for small molecules and atoms as found in all solids. The temperatures Θ_2 and Θ_1 correspond to linear and constant distribution of density of states with frequency, respectively.^{28,37} Figure 1b shows the results of the distribution of the density of states for Debye frequencies of the skeletal modes for water.

Knowing the Debye temperatures Θ_1 , Θ_2 , and Θ_3 , from a best fit of the experimental data, the skeletal heat capacities, $C_V(\text{skeletal})$, were calculated in the whole range of temperature. Then by adding the group vibration heat capacity to the calculated skeletal heat capacity, the total heat capacity at constant volume, $C_V(\text{total})$, was obtained in the solid state. Note that in eq 4 $C_V(\text{total})$ is equal to C_V . Next, $C_V(\text{total})$ was converted with eq 4 to heat capacity at constant pressure, C_p , which will be noted below as $C_p(\text{vib})$ or $C_p(\text{vibration})$. This calculated vibrational heat capacity, $C_p(\text{vib})$, was obtained for each type of poly(amino acid), $C_p(\text{vib}) \equiv C_p(i)$, from low to high temperature and then using eq 1, the total vibrational heat capacity, $C_p^{\text{silk}}(\text{vibration})$, was calculated for silk fibroin. This heat capacity, $C_p^{\text{silk}}(\text{vibration})$, serves as the baseline to judge additional contributions to the experimental apparent heat capacity of silk fibroin in the whole range of temperature for all states.

In the case of biopolymers such as silk and the silk–water system, the high-temperature range beyond the degradation temperature (for silk fibroin, starting at about 503.15 K (230 °C)) is still of value for discussions of thermal stability. At conventional scanning rates (up to about 20 °C/min for normal differential scanning calorimetry), silk degrades above 230 °C. However, using rapid scan nanoscale chip calorimetry, very fast rates, up to 10^6 K/s, are possible. These fast scan rates might

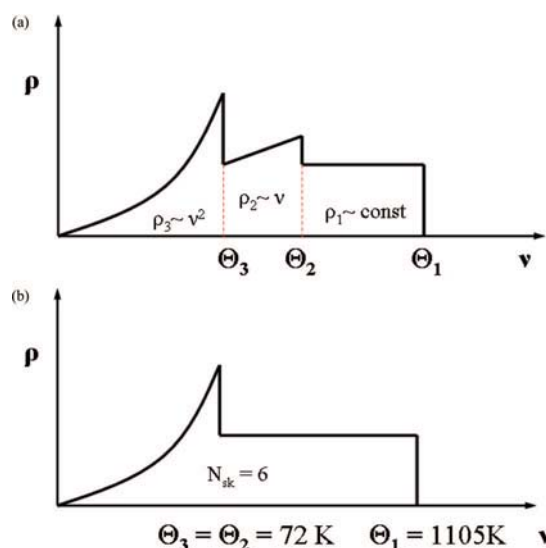


Figure 1. (a) General scheme of density of states (ρ) for Debye temperatures vs frequencies of the skeletal vibration modes. (b) Scheme of density of states (ρ) for Debye temperatures vs frequencies of the skeletal vibration modes for water.

prevent the degradation of silk, allowing higher temperature thermal processes to be explored. Therefore, it is of value to extend the heat capacity baseline data to higher temperatures beyond the glass transition, for ultimate comparison with results obtained through rapid scanning techniques.^{43,44}

The vibrational heat capacity of water, $C_p^{\text{water}}(\text{vibration})$, which is used in eq 11, was estimated in a similar method as for the solid state of each poly(amino acid). Similarly, based on the low-temperature experimental data for the heat capacity of glassy water measured by Suga and co-workers,⁴⁵ $C_p^{\text{water}}(\text{vibration})$ was evaluated. For the calculation of the vibrational heat capacity of water, the 9 degrees of freedom resulting from the 3 atoms of the molecule H_2O were separated into the 3 group vibrations and 6 skeletal vibrations. The group vibrational frequencies of glassy water were taken from normal-mode calculations based on the experimental infrared and Raman spectroscopy (O–H asymmetric stretch, with frequency 4685 K; H–O–H deformation with frequency 2365 K; and O–H symmetric stretch, with frequency 4685 K) as given in the literature.⁴⁶ The remaining 6 vibrational modes contribute to the skeletal heat capacity, which was calculated by fitting the experimental data with the general Tarasov equation (9). With the three Debye temperatures Θ_1 , Θ_2 , and Θ_3 resulting from the best fit of the experimental data and with parameters N_{sk} and A_0 , the $C_V^{\text{water}}(\text{skeletal})$ was estimated. Next by adding group vibration contribution, $C_V^{\text{water}}(\text{group})$, to the skeletal vibration contribution, $C_V^{\text{water}}(\text{skeletal})$, the total heat capacity of water at constant volume, $C_V^{\text{water}}(\text{total})$, was obtained. Finally, using eq 4, the heat capacity at constant pressure, $C_p^{\text{water}}(\text{vibration})$, for water was calculated. This vibrational heat capacity for water is used in the construction of the vibrational heat capacity of the silk–water system, $C_p^{\text{silk–water}}(\text{vibration})$, as shown in eq 11.

Calculation of the Heat Capacity for the Solid State of the Silk–Water System. The heat capacities of the solid silk–water system below T_g from vibrational motions were estimated from the linear combination of the molar or weight fractions of the vibrational heat capacity of silk, $C_p^{\text{silk}}(\text{vibration})$, and water, $C_p^{\text{water}}(\text{vibration})$, according to the formula

$$C_p^{\text{silk–water}}(\text{vibration}) = X_S C_p^{\text{silk}}(\text{vibration}) + X_W C_p^{\text{water}}(\text{vibration}) \quad (11)$$

where X_S and X_W are the molar fractions of silk and water, respectively, in the silk–water system. $C_p^{\text{silk–water}}(\text{vibration})$ [J/(K mol)] is the molar heat capacity of the mixture and is related to the specific heat capacity, $c_p^{\text{silk–water}}(\text{vibration})$ [J/(K g)] of the silk–water mixture given by

$$C_p^{\text{silk–water}}(\text{vibration}) = c_p^{\text{silk–water}}(\text{vibration})M \quad (12)$$

where M is the molar mass of the mixture and is calculated from

$$M = X_S M_w(\text{silk}) + X_W M_w(\text{water}) \quad (13)$$

where $M_w(\text{silk})$ and $M_w(\text{water})$ are the molar mass of silk and water, respectively.

For example, for the silk–water system containing 5.25 wt % water (i.e., weight fraction of water is 0.0525 and weight fraction of silk is 0.9475), the results of eqs 11–14 need the molar fractions of silk, $X_S = 0.000\,774\,9$, and water, $X_W = 0.999\,225$.⁴⁶ Using these values and the molar mass of silk and water, as $M_w(\text{silk}) = 419\,262$ g/mol and $M_w(\text{water}) = 18.0152$ g/mol, the molar mass of the mixture, M , was calculated from eq 13 as $M = 342\,892$ g/mol.

The method of estimation of the vibrational heat capacity of water, $C_p^{\text{water}}(\text{vibration})$, which is used in eq 11, was presented

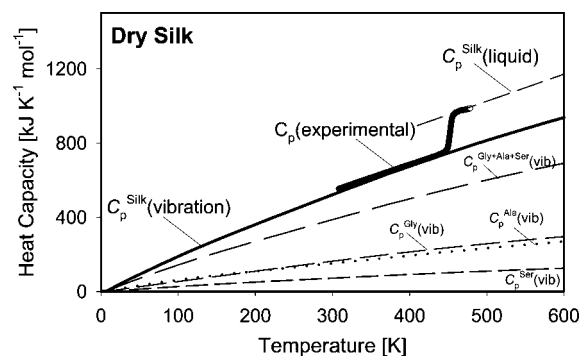


Figure 2. Comparison of the measured heat capacity of dry silk fibroin (open circles) to calculated vibrational heat capacity (thick solid curve) as functions of temperature. The vibrational heat capacities of the amino acids, glycine (Gly), alanine (Ala), and serine (Ser), and their sum, are indicated.

above together with the calculation for the solid state of poly(amino acid).

II. Results and Discussion

Figure 2 shows a comparison of calculated vibrational heat capacity of silk fibroin, $C_p^{\text{silk}}(\text{vibration})$ (solid curve), with the experimental heat capacity of dry amorphous *Bombyx mori* silk fibroin (open circles). The experimental reversing heat capacity was measured by temperature-modulated differential scanning calorimetry (TMDSC) as was already reported.^{20,21} The data show a step change in heat capacity as silk fibroin undergoes its glass transition at $T_g = 451.15$ K (178 °C).^{20,21} The vibrational heat capacity of silk, $C_p^{\text{silk}}(\text{vibration})$, was evaluated using the vibrational motion spectra of individual amino acids in silk fibroin. This vibrational heat capacity was constructed according to eq 1 using the vibrational C_p of the poly(amino acid)s from the Advanced Thermal Analysis System (ATHAS) Data Bank.³⁴ The vibrational C_p of the poly(amino acid)s collected in the Data Bank³⁴ were calculated early by Wunderlich and co-workers^{38,39} based on a fitting of the low-temperature experimental C_p . Knowing the numbers N_i of each type of amino acid in the silk fibroin and their corresponding vibrational heat capacity as a function of temperatures, the vibrational heat capacity of silk, $C_p^{\text{silk}}(\text{vibration})$, was calculated over the whole range of temperatures from 0.1 to 600 K. The computation has been carried out on the complete heavy chain sequence of 5263 amino acids and the light chain sequence of 263 of amino acids. The numbers N_i and compositions of the individual amino acids contained in *Bombyx mori* silk fibroin are presented in Table 1 and were taken from ref 11. For example, the 1593 molecules of alanine (Ala) in the heavy chain and the 37 molecules of alanine in the light chain of silk fibroin were taken into account to determine the alanine contribution to the total vibrational heat capacity of dry silk, $C_p^{\text{silk}}(\text{vibration})$. The molar masses of each amino acid, $M_w(i)$, contained in silk fibroin are also listed in Table 1 for convenience in converting the specific heat capacity into the molar heat capacity. In Figure 2 the vibrational heat capacities of the three amino acids, glycine, alanine, and serine, and their sum in relation to the total $C_p^{\text{silk}}(\text{vibration})$, are also shown (by dashed or dotted lines lying below the experimental data curve). These three amino acids account for ~85 mol % of the silk fibroin molecule. We observe that the sum of the vibrational heat capacities of glycine, alanine, and serine, gives ~75% of the total contribution to $C_p^{\text{silk}}(\text{vibration})$. Good agreement between the experimental data and the calculated vibrational heat capacity silk fibroin is observed below the glass transition temperature, T_g , of 451.15 K with an error $\pm 1\%$ between 380 and 435 K and with an error $\pm 3\%$ below 380 K. This agreement supports the conclusion that the only contribu-

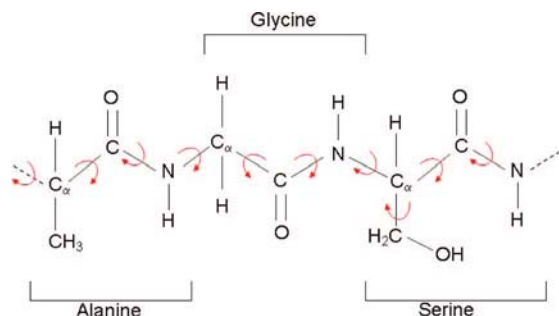


Figure 3. A portion of the polypeptide chain, showing the chemical structure of glycine, alanine, and serine. The arrows represent the bonds about which free rotation can occur resulting in change of conformation of the chain.

tion to the heat capacity below T_g for dry silk comes from the vibrational motion of the amino acid components.

The heat capacity of the liquid state, $C_p(\text{liquid})$, is more complicated to describe than that of the solid state. In the liquid state of polymers, the additional large-amplitude motions such as those due to conformational degrees of freedom, and anharmonicity should be considered beyond the harmonic vibrations. Calculations of the liquid heat capacity for a few synthetic and biological polymers, as well as the biopolymer–water system, have been analyzed in refs 31, 46, and 47. Empirically, it was found that the liquid heat capacity, $C_p(\text{liquid})$, is often a linear function of temperature. Using the best fit to experimental data, the liquid heat capacity of noncrystalline silk was estimated by Cebe and co-workers.^{20,21} In $\text{kJ}/(\text{mol K})$ the expression is written as

$$C_p^{\text{silk}}(\text{liquid}) = 297.676 + 1.455T \quad (14)$$

Experimental heat capacity data for noncrystalline silk fibroin are available only for a limited temperature range above the glass transition. At higher temperatures, the sample will crystallize and ultimately degrade.

Knowing the calculated vibration and liquid heat capacity of dry silk as baselines, we can quantitatively analyze the thermal properties of the experimental data. For example, we can estimate the change in heat capacity, or the “heat capacity increment”, at the temperature $T_g = 451.15 \text{ K}$ as $200\text{--}407 \text{ J}/(\text{mol K})$ between the vibrational and liquid baselines. According to Wunderlich,²⁸ each mobile unit in the chain of a polymer molecule contributes an amount of $11 \text{ J}/(\text{mol K})$ to the change of heat capacity at T_g . The value of $11 \text{ J}/(\text{mol K})$ is an average value and depends on the bonds which are naturally different between different kinds of atoms; more information can be found in ref 28. The ratio of our measured heat capacity increment to the contribution of a single mobile unit allows an estimate to be made of the total number of mobile units in noncrystalline silk fibroin. This ratio gives a total of 18 219 units of silk fibroin, which start to become mobile at the glass transition.

Above T_g , large-scale conformational changes occur in the mobile units of the molecular chain. Figure 3 depicts a portion of a polypeptide chain, showing three amino acid residues alanine, glycine, and serine. Each amino acid has at least three freely rotating bonds in the polypeptide chain backbone, which contribute to large-scale conformational changes occurring at T_g . The side groups may also contribute to the conformational degrees of freedom, depending upon side-group chemistry. For example, alanine and glycine have respectively a methyl or a hydrogen side group. Rotation of these groups will not change the overall polypeptide chain conformation. On the other hand, serine has the side group CH_2OH . Rotation about the bond connecting the α -carbon of serine to the CH_2 group will result in large-scale conformational change of the molecule. The red

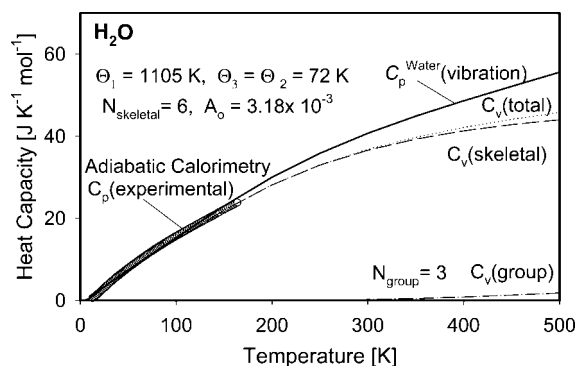


Figure 4. Comparison of the vibrational heat capacities for water from adiabatic calorimetry experiment (open circles) and calculated (solid and broken curves) as functions of temperature. The contributions from group and skeletal modes are indicated.

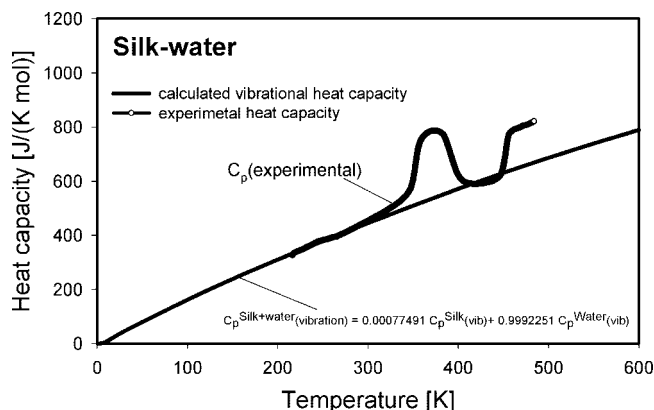


Figure 5. Comparison of the vibrational calculated heat capacities (heavy curve) and measured reversing heat capacities (open circles, for 5.25 wt % of water) of the silk–water system.

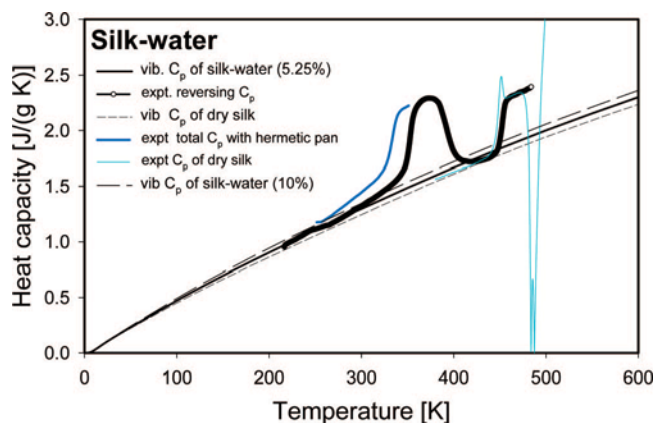


Figure 6. Comparison of the measured specific reversing (open circles) and total (black curve) heat capacities of the silk–water system from experimental data and calculated (heavy curve). Specific heat capacity of dry silk from experimental data (light blue curve) and calculated (dashed black curve).

arrows in Figure 3 show the bonds about which free rotation is able to occur when the silk fibroin undergoes its glass transition from the glassy to the liquid state.

We estimate the number of mobile units from the mol % of alanine, glycine, and serine, which together account for about 85% of the silk fibroin molecule. Counting three rotating bonds for Ala, three rotating bonds for Gly, and four rotating bonds for Ser, we calculate a sum of 14 841 rotating units for these three amino acids in one silk fibroin molecule. This number compares very favorably to 85% of 18 219 (85% of the

Table 2. Vibrational Heat Capacity of Silk Fibroin and Water

temp (K)	vibrational heat capacity of dry silk fibroin (kJ/(mol K))	temp (K)	vibrational heat capacity of water (J/(mol K))
0.1000	0.0000	0.1000	4.0000e-6 ^a
0.2000	0.0000	0.2000	1.2000e-5
0.3000	0.0000	0.3000	2.8000e-5
0.4000	0.0000	0.4000	5.6000e-5
0.5000	4.0000e-5	0.5000	1.0000e-4
0.6000	2.3900e-3	0.6000	1.6400e-4
0.7000	3.1450e-3	0.7000	2.5200e-4
0.8000	3.4010e-3	0.8000	3.6800e-4
0.9000	8.7160e-3	0.9000	5.1600e-4
1.0000	0.0111	1.0000	7.0000e-4
1.2000	0.0175	1.2000	1.1920e-3
1.4000	0.0286	1.4000	1.8760e-3
1.6000	0.0402	1.6000	2.7840e-3
1.8000	0.0602	1.8000	3.9480e-3
2.0000	0.0803	2.0000	5.4000e-3
3.0000	0.2753	3.0000	0.0181
4.0000	0.6492	4.0000	0.0430
5.0000	1.2649	5.0000	0.0839
6.0000	2.1610	6.0000	0.1445
7.0000	3.3525	7.0000	0.2270
8.0000	4.8304	8.0000	0.3317
9.0000	6.5515	9.0000	0.4572
10.0000	8.4717	10.0000	0.6006
15.0000	19.5907	15.0000	1.4706
20.0000	31.1307	20.0000	2.4004
25.0000	42.2120	25.0000	3.2972
30.0000	52.8312	30.0000	4.1558
40.0000	73.1966	40.0000	5.7988
50.0000	92.9942	50.0000	7.3925
60.0000	112.5375	60.0000	8.9625
70.0000	131.9875	70.0000	10.5210
80.0000	151.2865	80.0000	12.0810
90.0000	170.2719	90.0000	13.6550
100.0000	189.0787	100.0000	15.2550
110.0000	207.5905	110.0000	16.8340
120.0000	225.7641	120.0000	18.4030
130.0000	243.5348	130.0000	19.9570
140.0000	261.0056	140.0000	21.4910
150.0000	278.1530	150.0000	22.9990
160.0000	295.1541	160.0000	24.4670
170.0000	311.7435	170.0000	25.9020
180.0000	328.4586	180.0000	27.3010
190.0000	344.9152	190.0000	28.6600
200.0000	361.2884	200.0000	29.9770
210.0000	377.3343	210.0000	31.2330
220.0000	393.6876	220.0000	32.4460
230.0000	409.7845	230.0000	33.6150
240.0000	425.8397	240.0000	34.7430
250.0000	441.9357	250.0000	35.8310
260.0000	457.9649	260.0000	36.8740
270.0000	473.7921	270.0000	37.8800
273.1500	478.8283	273.1500	38.1860
280.0000	489.8122	280.0000	38.8520
290.0000	505.6815	290.0000	39.7910
298.1500	518.6911	298.1500	40.5320
300.0000	521.5082	300.0000	40.7000
310.0000	537.3747	310.0000	41.5820
320.0000	553.3779	320.0000	42.4390
330.0000	568.8505	330.0000	43.2720
340.0000	584.2873	340.0000	44.0840
350.0000	599.6193	350.0000	44.8760
360.0000	614.8824	360.0000	45.6530
370.0000	631.6035	370.0000	46.4150
380.0000	645.2078	380.0000	47.1630
390.0000	659.9732	390.0000	47.8980
400.0000	674.9161	400.0000	48.6220
410.0000	689.4970	410.0000	49.3380
420.0000	703.8584	420.0000	50.0470
430.0000	718.3254	430.0000	50.7480
440.0000	732.3913	440.0000	51.4440
450.0000	746.3587	450.0000	52.1360
460.0000	760.2171	460.0000	52.8250
470.0000	774.0250	470.0000	53.5130
480.0000	787.4212	480.0000	54.1990
490.0000	800.9117	490.0000	54.8860
500.0000	813.9374	500.0000	55.5730
510.0000	826.7540	510.0000	56.2630
520.0000	839.5220	520.0000	56.9550
530.0000	852.1793	530.0000	57.6520
540.0000	864.6989	540.0000	58.3540
550.0000	877.0873	550.0000	59.0630
560.0000	889.6590	560.0000	59.7790
570.0000	901.7529	570.0000	60.5030
580.0000	913.7337	580.0000	61.2370
590.0000	925.5856	590.0000	61.9810
600.0000	937.5871	600.0000	62.7370

^a Read as 4.0000×10^{-6} .

estimated total number of units contributing to the heat capacity increment at T_g), which result is 15 486. We conclude that the change in heat capacity at T_g of dry silk fibroin corresponds to the change anticipated for the fully noncrystalline material in our silk.

In order to evaluate the vibrational heat capacity of the silk–water system from the sum of two components of silk and water, the vibrational heat capacity of water should also be known.

Next, Figure 4 displays the evaluation of the calculated vibrational heat capacity of water from the fitting of the low-temperature experimental data. The estimation of $C_p^{\text{water}}(\text{vibration})$ was performed using a similar scheme of calculation as for each of the amino acids of silk. The results of the calculated vibrational heat capacity of water, $C_p^{\text{water}}(\text{vibration})$, are compared with the low temperature, experimental heat capacity, $C_p(\text{experimental})$, from adiabatic calorimetry in Figure 4. The comparison of the results shows that the only contribution into the experimental heat capacity at low-temperature results from the vibration motion of water. The major contribution to the vibrational heat capacity comes from the later, skeletal contribution, as is usually observed for the solid state of small molecules. This skeletal heat capacity was estimated using the Debye temperatures $\Theta_3 = 72.4$ K, $\Theta_2 = 72.4$ K, and $\Theta_1 = 1105.5$ K from the best fit to eq 9, using as the number of skeletal vibrations, $N_{\text{sk}} = 6$, and the value of $A_0 = 0.00318$, as indicated in Figure 4. From results of the best fit, Θ_2 is equal to Θ_3 , and this suggests that there is no two-dimensional contribution into the vibrational spectrum in water. Only very little contribution is observed from the three modes, $N_{\text{gr}} = 3$ of group vibrations, $C_v^{\text{water}}(\text{group})$, into the total vibration, $C_p^{\text{water}}(\text{vibration})$, in the region of high temperatures as shown in Figure 4.

The vibrational calculated heat capacity of the silk–water system was estimated on the basis of the linear combination of fractions of the vibrational heat capacities of both dry silk and water using eq 11. Figure 5 shows the comparison of the calculated vibrational heat capacity of the silk–water system with the experimental data of the reversing heat capacity of the of the silk with 5.25 wt % water. The experimental heat capacity was calibrated as previously described in ref 21. The $C_p^{\text{silk-water}}(\text{vibration})$ was calculated from the molar fraction, $X_s = 0.0077491$ and heat capacity of the solid, $C_p^{\text{silk}}(\text{vibration})$ for silk, and with molar fraction, $X_w = 0.9992251$ and heat capacity of the solid, $C_p^{\text{water}}(\text{vibration})$ for water. The molar mass of this mixture is $M = 342.892$ g/mol, as was already calculated from eq 13. Now, the vibrational heat capacity of the silk–water system, $C_p^{\text{silk-water}}(\text{vibration})$, can serve as a baseline for the quantitative thermal analysis of the experimental heat capacity of silk fibroin with water present for a whole range of temperatures. In Figure 5 we observe that below 300 K both the vibrational and experimental C_p are the same. The deviation between them starts above 300 K and gradually increases due to the glass transition relaxation process which occurs at 350 K in plasticized silk containing 5.25 wt % (0.9992251 mole fraction) of bound water in the system. This bound water content is typical of silk films cast from water solutions which are subsequently dried under vacuum. The bound water content was determined using thermogravimetry. Since the experimental measurements of the reversing heat capacity by TMDSC were not performed using hermetic pans, the examined system lost its water. After the glass transition of the silk–water system was completed, the reversing heat capacity in Figure 5 decreases due to evaporation of water to a level that is, as expected, even below the vibrational baseline heat capacity for the silk–water system. During the continuation of heating, the experimental C_p increases again, rising above $C_p^{\text{silk-water}}(\text{vibration})$ due to the

glass transition process of the now-dry silk which occurs at 451.15 K (178 °C).

Figure 6 is a comparison of several experimental and calculated vibrational heat capacities: the experimental specific reversing heat capacity of the silk–water system (open circles, 5.25 wt % of water), the experimental specific heat capacity of the dry silk, and additionally the experimental specific total heat capacity of silk with 10 wt % of water (solid line) from standard DSC using hermetic pan, together with their baseline vibrational heat capacities. It should be noted that the relationship between the specific heat capacity, c_p in [J/(K g)], and the molar heat capacity, C_p in [J/(K mol)], is in accordance with the relationship given by eq 12. The corresponding molar mass of dry silk ($M_w(\text{silk}) = 419\,262$ g/mol) and the molar mass of the mixture of silk with 5.25 and 10 wt % of water ($M = 342.892$ g/mol and $M = 180.110$ g/mol) (according to eq 13) should be known. Comparing data in Figure 6 makes it clear that the heat capacity of silk with 5.25 wt % water (open circles) has reached the level of the vibrational heat capacity of the silk–water system before T_g at 350 K and before evaporation of water starts. After the evaporation of water, during the continuation of the heating process, the experimental heat capacity of the initially partially hydrated silk–water system has reached the level of the calculated vibrational heat capacity of dry silk. With this example we can quantitatively analyze the sample by tracing the changes of heat capacity of the silk–water mixture due to the process of the evaporation of water.

In Figure 6, the experimental data of the total heat capacity of the silk with 10 wt % of water from standard DSC with hermetic pans together with the vibrational heat capacity is presented only for comparison and not for any quantitative analysis. In short, the measurements were performed with a sample mass of ~ 6.4 mg using hermetic pans, the weights of which matched very well to the reference (633.28 mg) and to the sample (633.29 mg). The sample was heated from -50 to 80 °C at a heating rate of 5 K/min with no change of sample weight during this experiment. Based on this measurement of T_g (60 °C) from our data and using the phase diagram of the glass transition temperature of *Bombyx mori* silk fibroin and water from the literature,⁴⁸ the weight % of water in our investigated sample was estimated at approximately short 10%.

As in Figure 5, the $C_p^{\text{silk-water}}(\text{vibration})$ with 10 wt % water was calculated using the molar fraction, $X_S = 0.000387$, and heat capacity of the solid, $C_p^{\text{silk}}(\text{vibration})$ for silk, and with molar fraction, $X_W = 0.999\,613\,4$, and heat capacity of the solid, $C_p^{\text{water}}(\text{vibration})$ for water. The molar mass of this mixture is $M = 180.110$ g/mol as already was estimated. Results of the calculated $C_p^{\text{silk-water}}(\text{vibration})$ with 10 wt % water fit very well to the entire series of the calculated vibrational heat capacities presented in Figure 6. It should be noted that in this case the experimental heat capacity in Figure 6 was calibrated only internally, and more quantitative data will be presented in the forthcoming paper. Results of total heat capacity of silk with 10 wt % water from standard DSC shows the glass transition occurring at a much lower temperature (333 K) than from measurements of the reversing C_p from TMDSC (350 K) using the nonhermetic pans. Both sets of data agree with the results from the phase diagram of T_g in dependence on water content in ref 48.

From comparison of the total heat capacity (light thin line) and reversing heat capacity (open circles) in the glass transition region of dry silk in Figure 6, several additional features are revealed in the total heat capacity curve, at and above the glass transition. First, there is a small enthalpy peak on the high temperature side of the glass transition, related to nonreversing processes such as physical aging. Immediately following the step at T_g , there is a strong cold crystallization peak. Above

this temperature, but not shown in Figure 6, are processes relating to degradation. The full data of the total heat capacity of dry silk have already been presented and discussed in refs 20 and 21.

The vibrational heat capacities of silk fibroin, determined in this work, and of water are listed in Table 2. These data will be added into the ATHAS Data Bank collection³⁴ as a permanent resource for the scientific community.

III. Conclusions

The heat capacities in the solid state of *B. mori* silk fibroin with and without water have been determined based on the contribution of vibrational motions of the components: poly(amino acid)s and water, as presented in Figures 2, 4, 5, and 6. The heat capacities, C_p , of dry silk and silk–water were linked to their vibrational spectra. The fully noncrystalline dry silk has a glass transition at 451.15 K (178 °C). The heat capacity of the solid silk–water system, below the glass transition, was estimated from a sum of linear combinations of the molar fractions of the vibrational C_p of dry silk and glassy water. Below the glass transition, contributions into the experimental heat capacity of solid silk and the silk–water system come only from the vibrational motions. The heat capacity of the amorphous sample increases again beyond the vibrational limit when approaching the glass transition due to the large-amplitude motion. The liquid heat capacity of noncrystalline dry silk, as presented by a linear function of temperature, fits well in the range of measurement. Depending on interest, this can be used as a reference baseline for quantitative thermal analysis of this biomaterial. With the C_p baselines of the solid and liquid states, the experimental heat capacity of dry silk was discussed in the glass transition region.

For the noncrystalline dry silk, the liquid heat capacity estimation based on vibrational, conformational, and external contributions will be the subject of a forthcoming investigation. Also, research based on present results on the silk–water system above T_g , and based on the differences between experimental and vibrational heat capacities, will provide quantitative information about the conformational heat capacities from chains of silk interacting with water and thus help in understanding the formation process of the silk fibroin system.

Acknowledgment. The work reported herein was conducted at Tufts University and was supported by the National Science Foundation, Polymers Program of the Division of Materials Research, through Grant DMR-0602473 and by European Union Grant (MIRG-CT-2006036558).

References and Notes

- (1) Kaplan, D. L.; Adams, W. W.; Farmer, B.; Viney, C., Eds. *Silk Polymers: Materials Science and Biotechnology*; ACS Symposium Series 544; American Chemical Society: Washington, DC, 1994.
- (2) McGrath, K.; Kaplan, D. L., Eds. *Protein-Based Materials*; Birkhauser Press: Boston, MA, 1996.
- (3) Altman, G. H.; Diaz, F.; Jakuba, C.; Calabro, T.; Horan, R. L.; Chen, J. S.; Lu, H.; Richmond, J.; Kaplan, D. L. *Biomaterials* **2003**, *24*, 401.
- (4) Chen, X.; Knight, D. P.; Shao, Z. Z.; Vollrath, F. *Polymer* **2001**, *42*, 9969.
- (5) Ishida, M.; Asakura, T.; Yokoi, M.; Saito, H. *Macromolecules* **1990**, *23*, 88.
- (6) Motta, A.; Fambri, L.; Migliaresi, C. *Macromol. Chem. Phys.* **2002**, *203*, 1658.
- (7) Foo, C. W. P.; Kaplan, D. L. *Adv. Drug Delivery Rev.* **2002**, *54*, 1131.
- (8) Agarwal, N.; Hoagland, D. A.; Farris, R. J. *J. Appl. Polym. Sci.* **1997**, *63*, 401.
- (9) Tretinnikov, O. N.; Tamada, Y. *Langmuir* **2001**, *17*, 7406.
- (10) Kim, Y. S.; Dong, L. M.; Hickner, M. A.; Glass, T. E.; Webb, V.; McGrath, J. E. *Macromolecules* **2003**, *36*, 6281.
- (11) Swiss-Prot Protein database on the Internet.

- (12) Kaplan, D. L.; Adams, W. W.; Farmer, B.; Viney, C., Eds. *Silk Polymers: Materials Science and Biotechnology*; ACS Symposium Series 544; American Chemical Society: Washington, DC, 1994.
- (13) Lee, K. Y.; Ha, W. S. *Polymer* **1999**, *40*, 4131.
- (14) Valluzzi, R.; Gido, S. P.; Murayama, K.; Tomida, M. *Biochemistry* **1997**, *42*, 705.
- (15) Valluzzi, R.; Gido, S. P.; Zhang, W. P.; Muller, W. S.; Kaplan, D. L. *Macromolecules* **1996**, *29*, 8606.
- (16) Agarwal, N.; Hoagland, D. A.; Farris, R. J. *J. Appl. Polym. Sci.* **1997**, *63*, 401.
- (17) Mijovic, J.; Bian, Y.; Gross, R. A.; Chen, B. *Macromolecules* **2005**, *38*, 10812.
- (18) Drummy, L. F.; Phillips, D. M.; Stone, M. O.; Farmer, B. L.; Naik, R. R. *Biomacromolecules* **2005**, *6*, 3328.
- (19) Wang, Y. Z.; Kim, H. J.; Vunjak-Novakovic, G.; Kaplan, D. L. *Biomaterials* **2006**, *27*, 6064.
- (20) Hu, X.; Kaplan, D. L.; Cebe, P. *Macromolecules* **2006**, *39*, 6161.
- (21) Hu, X.; Kaplan, D. L.; Cebe, P. *Thermochim. Acta* **2007**, *461*, 137.
- (22) Huang, J.; Foo, C. W. P.; Kaplan, D. L. *Polym. Rev.* **2007**, *47*, 29.
- (23) Hu, X.; Cebe, P. *Am. Chem. Soc. Div Polym. Mater.: Sci. Eng. Prepr.* **2005**, *93*, 652.
- (24) Matsumoto, A.; Chen, J.; Collette, A. L.; Kim, U. J.; Altman, G. H.; Cebe, P.; Kaplan, D. L. *J. Phys. Chem. B* **2006**, *110*, 21630.
- (25) Hu, X.; Kaplan, D. L.; Cebe, P. *Macromolecules* **2008**, *41*.
- (26) Yamane, T.; Umemura, K.; Nakazawa, Y.; Asakura, T. *Macromolecules* **2003**, *36*, 6766.
- (27) Wunderlich, B. *Pure Appl. Chem.* **1995**, *67*, 1019.
- (28) Wunderlich, B. *Thermal Analysis of Polymeric Materials*; Springer-Verlag: Berlin, 2005.
- (29) Wunderlich, B. *Prog. Polym. Sci.* **2003**, *28*, 383.
- (30) Pyda, M.; Wunderlich, B. *Macromolecules* **2005**, *38*, 10472.
- (31) Pyda, M. *Macromolecules* **2002**, *35*, 4009.
- (32) Fung, B. M.; Cox, J. A. *Biopolymers* **1979**, *18*, 489.
- (33) Uryash, V. F.; Sevast'yonov, V. I.; Kokurina, N.; Yu.; Porunova, Yu. V.; Perova, N. V.; Faminskaya, L. A. *Russ. J. Gen. Chem.* **2006**, *76*, 1363.
- (34) Pyda, M., Ed.; ATHAS Data Bank, **2007**; <http://athas.prz.edu.pl> or <http://web.utk.edu/~athas/>.
- (35) Magoshi, J.; Magoshi, Y.; Nakamura, S.; Kasai, N.; Kakudo, M. *J. Polym. Sci., Polym. Phys.* **1977**, *15*, 1675.
- (36) Motta, A.; Fambri, L.; Migliaresi, C.; Macromol, *Chem. Phys.* **2002**, *203*, 1658.
- (37) Pyda, M.; Bartkowiak, M.; Wunderlich, B. *J. Therm. Anal.* **1998**, *51*, 631.
- (38) Roles, A. K.; Xenopoulos, A.; Wunderlich, B. *Biopolymers* **1991**, *31*, 477.
- (39) Roles, A. K.; Xenopoulos, A.; Wunderlich, B. *Biopolymers* **1993**, *33*, 753.
- (40) Di Lorenzo, M. L.; Zhang, G.; Pyda, M.; Wunderlich, B. *J. Polym. Sci., Part B: Polym. Phys.* **1999**, *37*, 2093.
- (41) Debye, P. *Ann. Phys.* **1912**, *39*, 789.
- (42) Tarasov, V. V. *Zh. Fiz. Khim.* **1950**, *24*, 111.
- (43) Miniakov, A. A.; Schick, C. *Rev. Sci. Instrum.* **2007**, *78*, 111.
- (44) Ray, V. V.; Bathia, A. K.; Schick, C. *Polymer* **2007**, *48*, 2404.
- (45) Sugisaki, M.; Suga, H.; Seki, S. *Bull. Chem. Soc. Jpn.* **1968**, *41*, 2591.
- (46) Pyda, M. *J. Polym. Sci., Part B: Polym. Phys.* **2001**, *39*, 3038.
- (47) Pyda, M. Quantitative Thermal Analysis of Carbohydrate-water Systems. In *The Nature of Biological Systems as Revealed by Thermal Methods*; Lorinczy, D., Ed.; Kluwer Academic Publisher: Amsterdam, 2004; pp 307–333.
- (48) Agarwal, N.; Hoagland, D. A.; Farris, R. J. *J. Appl. Polym. Sci.* **1997**, *63*, 401.

MA8003357